FIELD-ORIENTED CONTROL OF INDUCTION MOTOR APPLIED VIA INVERTER H BY PSPWM AND PDPWM

Lotfi El M'barki , Moez Ayadi & Rafik Neji

University of Sfax, Tunisia
Laboratory of Electronic and Information Technology Sfax (LETI)
Electric Vehicle and Power Electronics Group (VEEP)
Email: indtechtunisie@yahoo.fr, moez.ayadi@enis.rnu.tn, Rafik.neji@enis.rnu.tn

ABSTRACT

About the past half century, the three phases asynchronous motor has been the motor of choice in industrial applications as power electronics, can be to control its output performance. Since use, the DC motor was largely employed, before of easy control of torque and speed. The asynchronous machine utilizes few internal parts that need maintenance or replacement. The control-oriented vector of rotor flux of voltage, applied to the asynchronous machine can transform the expression of electromagnetic torque of the asynchronous machine to nearly comparable to that of DC motor. This paper presents an application of control-oriented vector of rotor flux of asynchronous machine, applied a comparison by two PWM strategies, for multilevel-cascaded inverter PSPWM and multilevel-cascaded inverter PDPWM. The simulation of the proposed controllers applied to the asynchronous machine drive is implemented in MATLAB/SIMULINK.

Keywords: *Asynchronous machine, Control-oriented vector of rotor flux, Cascaded multilevel inverter PSPWM, Cascaded multilevel inverter PDPWM, Harmonic distortion, Junction temperature*

1. INTRODUCTION

In the last decade, many researches were continued for the ordering of the IM (induction motor). The plurality methods are based on the model reference condition system of the control-oriented vector of rotor flux. The induction motor accepted in variable speed drives due to its distinguished advantages of easy construction [1-3]. The asynchronous machine uses few internal parts that need maintenance or replacement. The control-oriented vector of rotor flux of voltage applied to the asynchronous machine can transform the expression of electromagnetic torque of the asynchronous machine to practically the torque of the D.C machine. The technique model of the asynchronous machine is resulted by transforming the three phase expressions into two-phase expressions [5-11]. In this work, the decoupling V_{ds} and V_{qs} to control the flux particularly in the course of the component I_{ds} and I_{qs}, which rejoinder to the suggestions of decoupling of the dependent excited D.C motor [18]. The estimators determine the couple, the junction temperature, rotor flux and the stator pulsation. The control of asynchronous machine, can transform the expression of electromagnetic torque of the asynchronous machine to nearly the torque of the DC machine. This paper presents an application of control-oriented vector of rotor flux of asynchronous machine, applied a comparison by two PWM (Pulse width modulation) strategies, for multilevel-cascaded inverter PSPWM (Phase Shifted PWM) and multilevel-cascaded inverter PDPWM (Phase Disposition PWM) [4]. Moreover, with multilevel inverter PWM and control-oriented vector of rotor flux, the voltage applied to the IM solicits a modulator stage. This stage adds to the signal processing (orders IGBTs of the inverter of the type H) time and consequently limits the reactions of the control system, and hence the torque and speed response time. The control-oriented vector of rotor flux of voltage, applied to the asynchronous machine is implemented in MATLAB/SIMULINK.

2. MATHEMATICAL MODEL OF ASYNCHRONOUS MACHINE

The technology of the asynchronous machine and their control-oriented vector of rotor flux require the use of a property system of modeling. Presently the most used is that of Park [9] [10] [14][15][18].

A dynamic model for an application of control-oriented vector of rotor flux of asynchronous machine, by choosing the tensions equations modeling of Park in the stator model are givens by the following equations:

$$V_{ds} = Rs\left(\sigma.\tau_S \frac{dI_{ds}}{dt} + I_{ds} - \sigma.\tau_S.\omega_S.I_{qs}\right) + Rs\left(\frac{\tau_S(1-\sigma)}{M}\frac{d\Phi_r}{dt}\right) \quad (1)$$

$$V_{qs} = Rs\left(\sigma.\tau_s \frac{dIqs}{dt} + I_{qs} + \sigma.\tau_s.\omega_s.I_{ds}\right) + Rs\left(\frac{\tau_S(1-\sigma)}{M}\omega_s.\Phi_r\right) \quad (2)$$

The equations of the currents by asynchronous machine in a reference related to the spinning vectorial control by oriented rotor flux pattern become.

$$I_{ds} = \frac{\tau_r}{M}\left(\frac{d\Phi r}{dt} + \frac{\Phi_r}{\tau_r}\right) \quad (3)$$

$$I_{qs} = \frac{Lr}{p.M.\Phi r}.Te \quad (4)$$

From equation (3), we deduce.

$$\Phi_r = \frac{M}{1+\tau_r.S} I_{ds} \quad (5)$$

By taking account of these relations, the electromagnetic can be written.

$$T_e - T_r = F\frac{\omega_m}{p} + \frac{J}{p}\frac{d\omega_m}{dt} \quad (6)$$

3. CASCADED MULTILEVEL CONVERTER

A cascaded multilevel converter PWM is poised as different H-bridges or commutation cells connected in series by phase as revealed in figure 3. For each single H-bridge, inverter includes two-arm and a DC source; each arm is carried of two IGBTs switches complementary [12]. The PWM output generates a pulse wave towards IGBTs with a duty cycle that is realized by the modulator; imply four pulses are generated for a two-arm bridge. The application of control-oriented vector of rotor flux of asynchronous machine, applied a comparison by two PWM strategies, for multilevel-cascaded inverter PSPWM and multilevel-cascaded inverter PDPWM [4].

3.1. Phase Shifted PWM

Figure 1, show the Phase Shifted Multi-carrier PWM system utilizes four carrier signals of the similar amplitude and frequency with are phase shifted by π/2. The cell for two switching is phase-shifted by π/2. The PSPWM strategy used by the comparison of carrying triangular fixes high frequency F_H, with one modulating variable low frequency F_L. The modulation frequency M_f defined for $M_f = F_H/ F_L$.

For the PSPWM, the modulation waveform has peak-to-peak amplitude A_m and the carrier waveform has peak-to-peak amplitude A_c.The modulation index Mi defined for $Mi = A_m/A_c$.

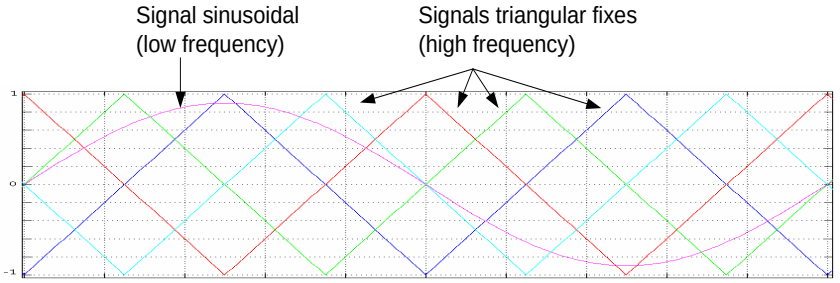

Figure 1. The triangular carrier's signals are compared with the sinusoidal modulating signal (PSPWM strategy)

3.2. Phase Disposition PWM

The figure 2, show the PDPWM method used by the comparison of carryings triangular fixes high frequency F_H, with one modulating variable low frequency F_L [13]. Through this process, all carriers are in phase as shown in figure 2. The output voltage is simulated PDPWM method, by modulation frequency M_f defined for: $M_f = F_H/ F_L$.

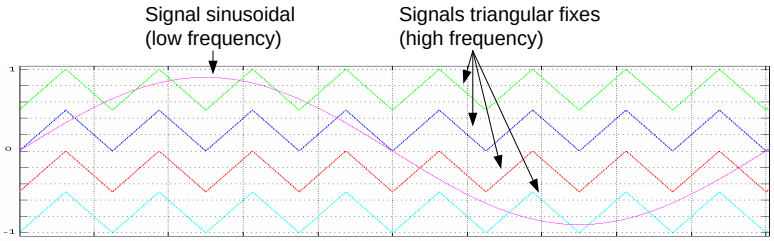

Figure 2. The triangular carrier's signals are compared with the sinusoidal modulating signal (PDPWM strategy)

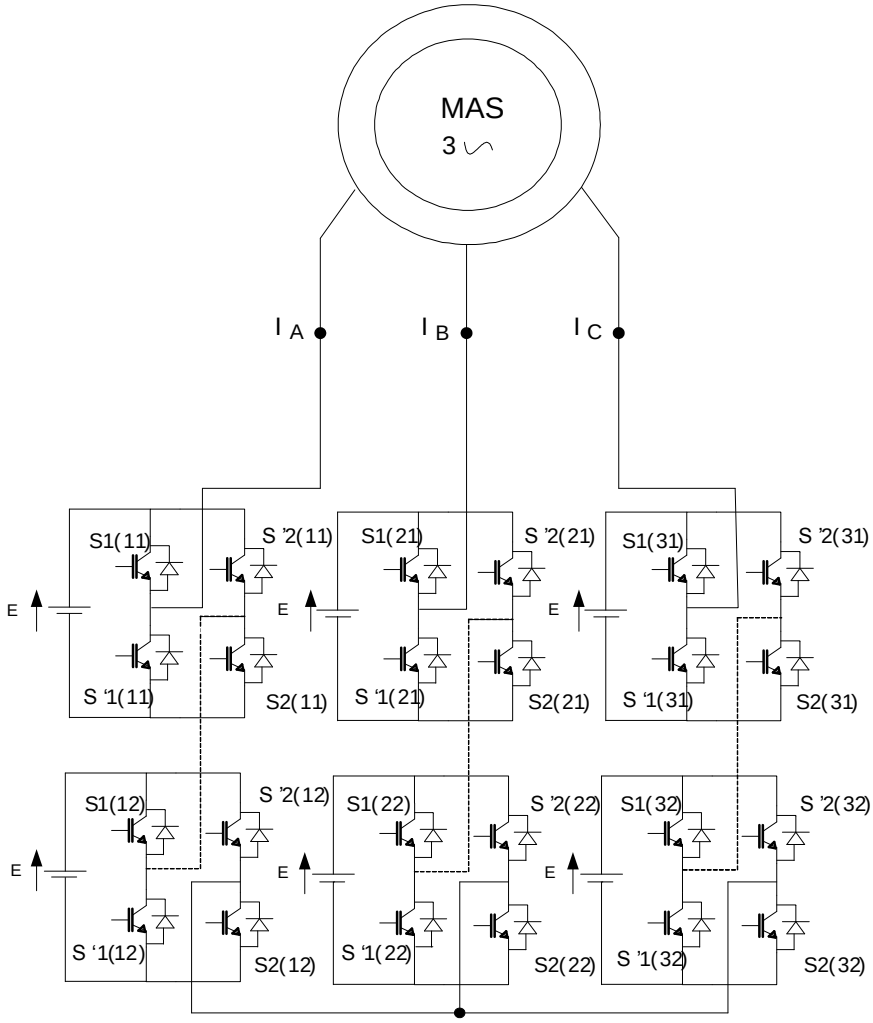

Figure 3. Three-phase cascaded multilevel inverter PWM of the type H

For the PDPWM, the modulation waveform has peak-to-peak amplitude A_m and the carrier waveform has peak-to-peak amplitude A_c. The modulation index Mi is defined for: $Mi=A_m/4A_c$.

The tensions V_A, V_B and V_C (in the figure 3), for multilevel-cascaded inverter PSPWM and multilevel-cascaded inverter PDPWM , are given by the following equation:

$$\begin{bmatrix} V_A \\ V_B \\ V_C \end{bmatrix} = \frac{E}{3}\begin{bmatrix} 2 & -1 & -1 \\ -1 & 2 & -1 \\ -1 & -1 & 2 \end{bmatrix}\begin{bmatrix} \sum_{j=1}^{2}\left[S_{1(1,j)} + S_{2(1,j)} - 1\right] \\ \sum_{j=1}^{2}\left[S_{1(2,j)} + S_{2(2,j)} - 1\right] \\ \sum_{j=1}^{2}\left[S_{1(3,j)} + S_{2(3,j)} - 1\right] \end{bmatrix} \quad (7)$$

4. THERMAL MODELLING OF THE POWER HYBRID MODULE

Literature proposes some approaches to construct thermal networks equivalent to a discretization of the heat equation. For example, the finite difference method (FDM) and the finite element method (FEM) are proposed.

In the case of vertical power devices, where the thickness L_{SI} is small compared to other dimensions, it is commonly considered that heat is generated at the top surface of silicon and flows uniformly along the x-axis (perpendicular to the silicon surface). So, the top surface is considered to be a geometrical boundary of the device at x = 0, where the input power P_0 (t) is assumed to be uniformly dissipated.

In our case we have chosen the (FEM) technique to develop the thermal model of the hybrid structure. Each material is represented by a simplified 1D thermal model. For the isolation and baseplate layer a modification have been introduced on the 1D model to take into account the thermal mutual between the different components.

The thermal investigation that was performed with the Semikron module SKM 75GB 123D (75A/1200V). The superposition technique [16-18] is used to develop the simplified thermal model of the hybrid structure. The method simply requires that for each independent heat source present, one test must be performed.

The literatures [16-18] shows the circuit networks corresponding to the IGBT thermal model used to estimate the thermal behavior of the IGBT in the module.

5. SIMULATION RESULTS AND DISCUSSION

The block diagram of control-oriented vector of rotor flux of asynchronous machine, applied a comparison by two PWM strategies, jointly with three-phase multilevel inverter block and thermal model, is shown in figure 4 [3-7].

For the rotor flux, the junction temperature, the torque and synchronisation speed are calculated directly the measured or estimated sizes. The stator current, I_{ds} and I_{qs} will be the variables of entry of an decoupling control of flux and torque.

Now we have; the equations $-\sigma.L_s.W_s.I_{qs}$, $\sigma.L_s.W_s.I_{ds}$ and $\frac{M}{Lr}.W_s\Phi_r$ are decoupled voltages in the figure 4.In this technique the flux Φr and torque Te are used as control references of machine and the stator two currents (ids, iqs) as command variables. With: $\Phi_r = \Phi_{dr}$, because with electric starting $\Phi_r = 0.Wb$, accordingly $\varphi_r = \Phi_r + 0.45$ (to carry out the starting of electric). The synchronisation speed ω_s is of writing according to the following equation.

$$Ws = p.\Omega + \frac{M}{\tau_r.\varphi_r}.I_{qs} \quad (8)$$

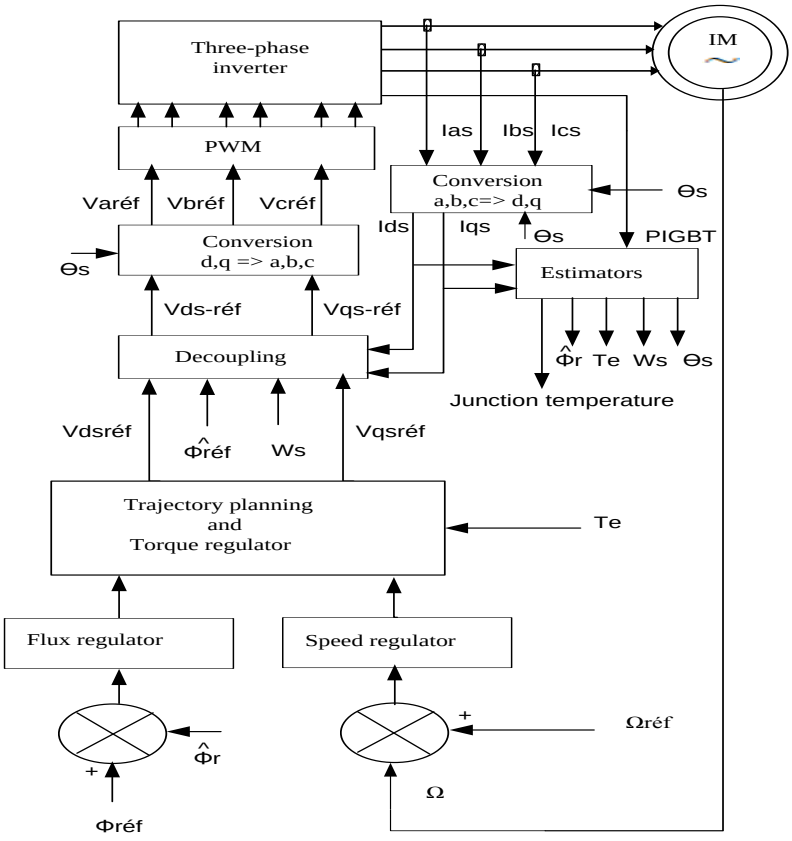

Figure 4. Block diagram of the proposed control of asynchronous motor.

Figure 5, show the reached steady state at t=1,03s, for the motor electromagnetic torque, in the two multilevel converter (PSPWM and PDPWM).

A zoom in the steady state shows the electromagnetic torque obtained by the multilevel inverter PSPWM oscillate 6 times by fundamental frequency. On the other hand, the electromagnetic torque obtained by the multilevel inverter PDPWM is constant (the torque ripples are much reduced) in the fundamental frequency. This last allows increasing the quality of operation motor.

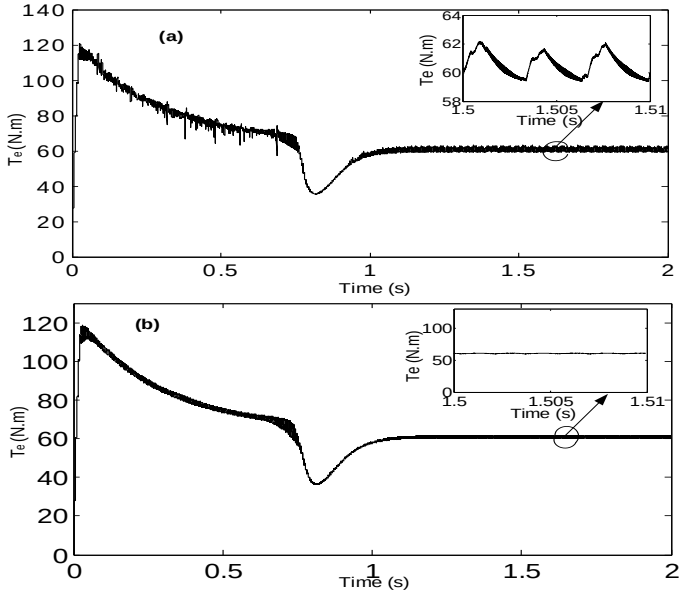

Figure 5. Electromagnetic torque evolution as a function of the time;
(a).obtained by multilevel inverter PSPWM and (b).obtained by multilevel inverter PDPWM

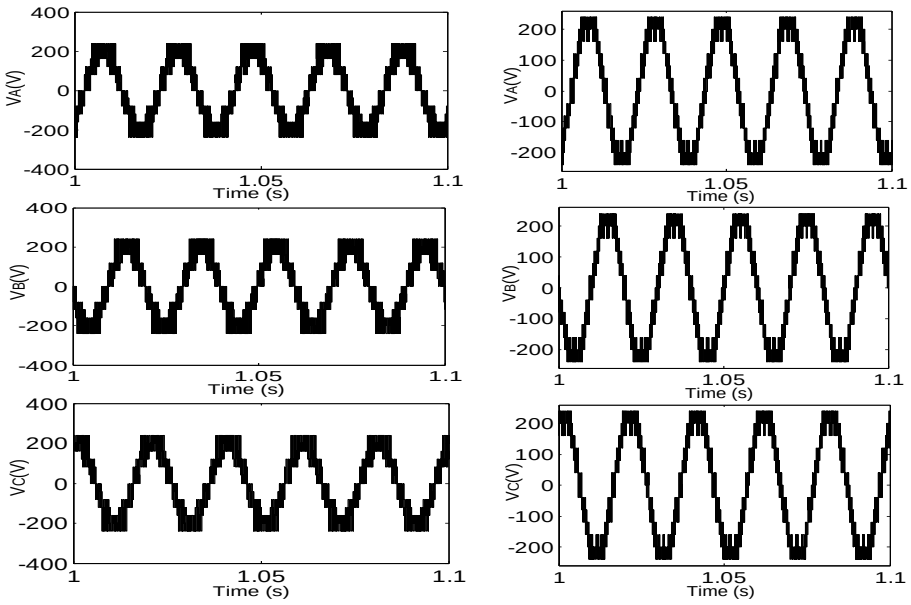

Figure 6. Output voltage (Modulation index Mi = 0.9 and modulation frequency M_f =200); (a).The output voltage of Inverter PSPWM and (b) The output voltage of Inverter PDPWM

Figure 6 (a) and figure 7 (a), shows the outputs voltages of multilevel inverter PSPWM with modulation index 0,9; THD_V value is 25,8% and fundamental frequency 50Hz with output voltage is 224V.

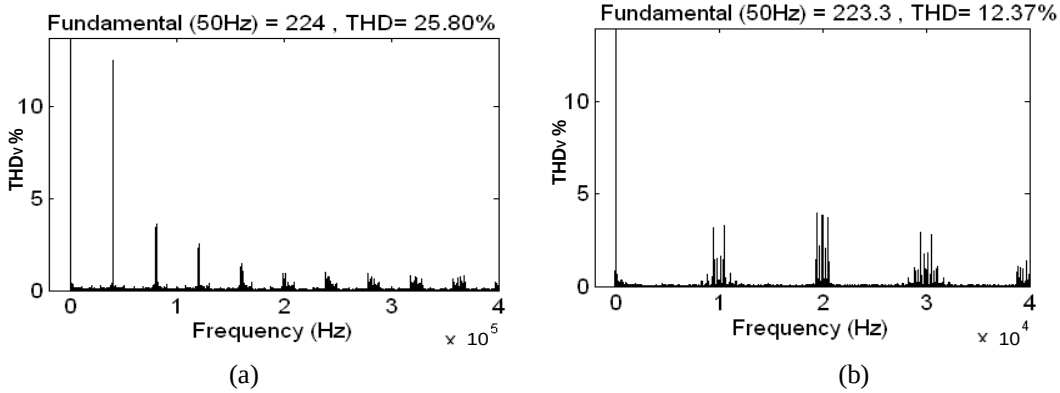

Figure 7. Harmonic spectrum voltage (Modulation index Mi = 0.9 and modulation frequency M_f =200); (a).PSPWM harmonic spectrum voltage and (b). PDPWM harmonic spectrum

Figure 6 (b) and figure 7 (b), shows the outputs voltages of multilevel inverter PDPWM with modulation index 0,9; THD_V value is 12,37% and fundamental frequency 50Hz with output voltage is 223,3V.

Figure 8 (a), shows the harmonic spectrum current of multilevel inverter PSPWM with modulation index 0,9 bay THDI value is 1,12%. Figure 8 (b), shows the harmonic spectrum current of multilevel inverter PDPWM with modulation index 0,9. The THDI value is 0,74%.

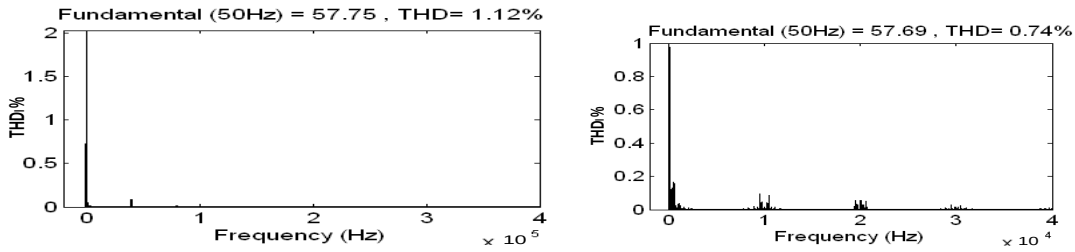

(a) (b)

Figure 8. Harmonic spectrum current (a1).obtained by multilevel inverter PSPWM and (a2).obtained by multilevel inverter PDPWM

Figure 9, gather at the same time the electric starting and ripples times for electromagnetic torque evolution as a function of the current. Special interest was focused on the stator current and the oscillations rate of the electromagnetic torque as functions of the qualities. The simulation, electromagnetic torque evolution as a function of the current, is obtained in the time [0 with 2s].

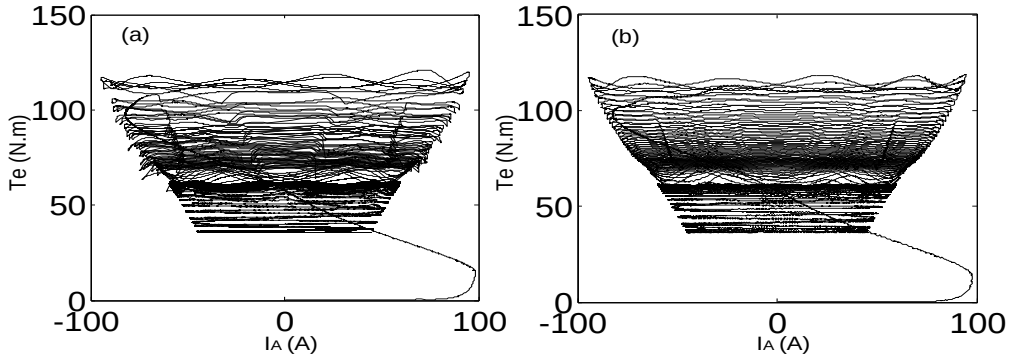

Figure 9. Electromagnetic torque evolution as a function of the current; (.a).obtained by multilevel inverter PSPWM and (b).obtained by multilevel inverter PDPWM

In order to estimate the junction temperature of the IGBT, figure 10 shows the evolution of the maximal junction temperature in the IGBT. In the thermal simulation two different inverters have been used; multilevel inverter PSPWM and multilevel inverter PDPWM. It is clear the IGBT junction temperature obtained by PSPWM lower of the junction temperature obtained by the PDPWM. For example, at a time equal to 0,15s, the IGBT junction temperature obtained by multilevel inverter PSPWM equal to 333K whereas the IGBT junction temperature obtained by PDPWM equal to 335.5K. These results shows, the utilization of the multilevel inverter PSPWM decrease the losses in semiconductors switches. The PSPWM can be used for very high power application, which needs low stress on power devices as IGBTs.

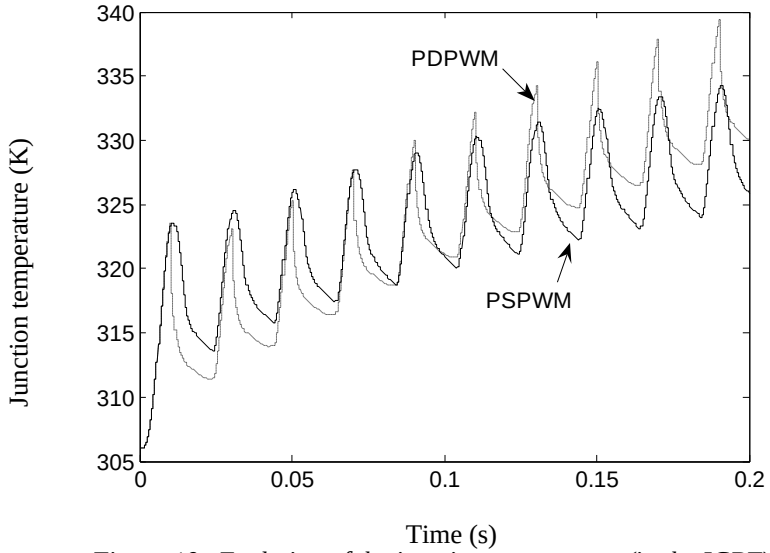

Figure 10. Evolution of the junction temperature (in the IGBT)

The simulation results from figure 6 to figure 10 display the desired behavior, with regard to the quality of the vector control IM obtained in the table 1.

Table 1. Apparent frequencies of the harmonics, junction temperature, and THD for multilevel inverters PSPWM and PDPWM

VECTOR CONTROL OF INDUCTION MACHINE	MULTILEVEL INVERTER PSPWM	MULTILEVEL INVERTER PDPWM
THDV %	25,80	12,37
THDI %	1,12	0,74
Fa (harmonic 1)	40 KHz	10 KHz
Fa (harmonic 2)	80 KHz	20 KHz
Fa (harmonic 3)	120 KHz	30 KHz
junction temperature in the IGBT (in the time 0.15s)	333 K	335.5 K

.

6. NOMENCLATURE

R_s: Stator resistance (1.4534 Ω)
R_r: Rotor resistance (1.4160 Ω)
V_{ds}, V_{qs}: d-axis and q-axis stator voltages
I_{ds}, I_{qs} : d-axis and q-axis stator currents
L_r: Rotor inductance (0.0143H)
L_s: Stator inductance (0.0144H)
M: Mutual inductance (0.0132H)
$\sigma = 1 - \frac{M^2}{Lr.Ls}$: Total leakage factor
$\tau_s = \frac{Ls}{Rs}$: Stator time constant
Φ_r: Rotor Flux
Φ_s : Stator flux
ω_s: Synchronisation speed
$\tau_r = \frac{Lr}{Rr}$: Rotor time constant
S: Laplace Operator
T_r: Load of torque (60N.m)
T_e: Electromagnetic Torque
F: Friction coefficient (0.014 kg.m² /S)
ω_m: Electromechanical angel speed of the motor
Ω : Mechanical rotor speed
J: Moment of inertia (0.311kg.m²)
p : Number of pole pairs in the motor (2)
F_p: Carrying frequency (10 KHz)
F_L : Fundamental frequency (50 Hz)
Fa: The apparent frequencies of the harmonics
E: Continuous voltage (120V)

7. OVERALL CONCLUSIONS

The association of asynchronous machine with a multi level inverter, is applied by comparison of two PWM strategies, was analyzed. A simulation study was used to back amelioration in the vectorial control of asynchronous machine and inverter PWM technique with better harmonic spectrum. Special interest was adjusted on the THD, the oscillations rate of the electromagnetic torque, the junction temperature and the stator current, as functions are determined by of the multilevel inverter quality. The diminution of the switch's commutation reduces losses in commutation then loss iron in the motor. The simulation results show high performances in the vectorial control of IM.

8. ACKNOWLEDGEMENTS

The authors would thank my colleagues in ENIS-Tunisia, in FSG-Tunisia, and in ESSTT-Tunisia for the helpful support in the work.

9. REFERENCES

[1]. Jon Are Suul, Marta Molinas, and Tore Undeland, " STATCOM - Based Indirect Torque Control of Induction Machines During Voltage Recovery After Grid Faults ", IEEE Transactions on power electronics, vol. 25, no. 5, May 2010,pp.1240-1250.

[2]. G. K. Singh, D. K. P. Singh, K. Nam and S. K. Lim, "A Simple Indirect Field-Oriented Control Scheme for Multiconverter-Fed Induction Motor", IEEE Transactions on industrial electronics, vol. 52, no. 6, December 2005, pp.1653-1659.

[3]. Gabriel Cimuca, Stefan Breban, Mircea M. Radulescu,Christophe Saudemont, and Benoit Robyns, "Design and Control Strategies of an Induction-Machine-Based Flywheel Energy Storage System Associated to a Variable-Speed Wind Generator", IEEE Transactions on energy conversion , vol.25,no.2,June 2010,pp.526-534.

[4]. Brendan Peter McGrath, and Donald Grahame Holmes, "Multicarrier PWM Strategies for Multilevel Inverters", IEEE Transactions on industrial electronics, vol. 49, no. 4, August 2002, pp.858-867.

[5]. Epaminondas D. Mitronikas, Athanasios N. Safacas, , and Emmanuel C. Tatakis," A New Stator Resistance Tuning Method for Stator-Flux-Oriented Vector-Controlled Induction Motor Drive", IEEE Transactions on industrial electronics, vol. 48, no. 6, December 2001, pp.1148-1157.

[6]. Julio C. Moreira, , and Thomas A. Lipo,"A New Method for Rotor Time Constant Tuning in Indirect Field Oriented Control", IEEE Transactions on power electronics, vol. 8, no.4.october 1993 ,pp.626-631.

[7]. Lazhar Ben-Brahim and Atsuo Kawamura, " A Fully Digitized Field-Oriented Controlled Induction Motor Drive Using Only Current Sensors", IEEE Transactions on industrial electronics, vol. 39, no. 3, Juner 1992, pp.241-249.

[8]. Yun Wei Li, Manish Pande, Navid R. Zargari, and Bin Wu, "DC-Link Current Minimization for High-Power Current-Source Motor Drives", IEEE Transactions on power electronics, vol. 24, no. 1, January 2009,pp.1240-1250,pp.232-240.

[9]. Rudolf S. Wieser, "Optimal Rotor Flux Regulation for Fast-Accelerating Induction Machines in the Field-Weakening Region", IEEE Transactions on industry applications, vol.34,no.5, September/October 1998 ,pp.1081-1087

[10]. Luiz Antonio de Souza Ribeiro, Cursino Brand˜ao Jacobina, Antonio Marcus Nogueira Lima, and Alexandre Cunha Oliveira"Parameter Sensitivity of MRAC Models Employed in IFO-Controlled AC Motor Drive", IEEE Transactions on industrial electronics, vol. 44, no. 4, August 1997, pp.536-545.

[11]. Keith A. Corzine, "A Hysteresis Current-Regulated Control for Multi-Level Drives", IEEE Transactions on energy conversion,vol.15,no.2,June 2000,pp.169-175.

[12]. A. Pe´rez-Toma´s, X. Jorda`, P. Godignon, J.L. Ga´lvez, M. Vellvehı´, J. Milla´n," IGBT gate driver IC with full-bridge output stage using a modified standard CMOS process", Microelectronics Journal 35 (2004),pp. 659–666.

[13]. B.Shanthi and S.P.Natarajan, "Carrier overlapping PWM methods for single phase cascaded five level inverter ", International journal of sciences and techniques of automatic control & computer engineering, CEM, December 2008,pp.590-601.

[14]. A A Ansari, D M Deshpande, "Mathematical Model of Asynchronous Machine in MATLAB Simulink",International Journal of Engineering Science and Technology, Vol. 2(5), 2010, pp.1260-1267.

[15]. Robert D.Lorenz and Donald B.Lawson , "A Simplified Approach to Continuous On-Line Tuning of Field-Oriented Induction Machine Drives", IEEE Transactions on industry applications, vol.26,no.3,May/June 1990 ,pp.420-424.

[16]. Moez Ayadi, Mohamed Amine Fakhfakh, Moez Ghariani and Rafik Neji, " Electrothermal modeling of hybrid power", Microelectronics International, vol. 27. n. 3, August 2010, pp. 170-177.

[17]. Moez Ayadi, Mohamed Amine Fakhfakh, Moez Ghariani and Rafik Nej, ''Electro-Thermal Simulation of a Three Phase Inverter with Cooling '', Journal of Modelling and Simulation of Systems, vol. 1. n. 3, 2010, June 2010, pp. 163-170.

[18]. [18] M. Ayadi, L. El M'barki, M. A. Fakhfakh, M. Ghariani, R. Neji,'' A Comparison of PWM Strategies for Multilevel Cascaded and Classical Inverters Applied to the Vectorial Control of Asynchronous Machine '', International Review of Electrical Engineering (I.R.E.E.), Vol. 5, N. 5, September-October 2010, pp.2106-2114